

Applications of Surface Analytical Techniques in Corrosion Research (Mainly High Temperature Corrosion)

Uporaba površinskih analiznih tehnik v raziskavah korozije

H. Vieffhaus¹, Max-Planck-Institut, Düsseldorf, Germany

Prejem rokopisa - received: 1996-10-01; sprejem za objavo - accepted for publication: 1996-11-04

The application of materials under various environmental conditions strongly depends on the corrosion properties of those materials. This is in particularly true for high temperature materials to be used in power plants, petrochemical, chemical and automobil industry, where during application high temperatures and aggressive environments may cause great problems. At low temperatures the corrosion of metals is often inhibited by a passive layer on the metal surface. To understand the phenomenon of passivity the formation and nature of this surface film, quite often only a few nm's thick, has to be characterized. Corrosion protecting layers on high temperature materials, either grown during application or precovered before application, have a much larger thickness. In order to study the growth mechanisms, nature and properties of corrosion protecting layers thin films have to be characterized spreading over a quite large range of thicknesses, from a few nm's for the passive layers up to several μm 's for the protecting layers on high temperature materials. Different methods for thin film analysis using surface analytical methods will be presented and illustrated by examples from different areas of corrosion research.

Key words: corrosion, high temperature corrosion, surface analytical techniques

Uporaba materialov v različnih okoljih zavisi od njihovih korozijskih lastnosti. To je posebno pomembno pri uporabi materialov pri visokih temperaturah in agresivnih medijih npr. v elektrarnah, petrokemijski, kemijski in avtomobilski industriji, kjer lahko pride do hudih industrijskih havarij. Pri nizkih temperaturah se na površini kovin tvori tanka pasivna plast, ki zavira korozijo. Razumevanje pojave nastanka in narave tanke pasivne plasti, ponavadi debele le nekaj nanometrov je mogoče samo s karakterizacijo teh plasti. Protikorozijske zaščitne plasti materialov, ki se uporabljajo pri visokih temperaturah in nastajajo med samo uporabo ali pa so bile predhodno nanosene, so debelejšje. Študij mehanizma rasti, narave in lastnosti protikorozijskih prevlek je mogoč z raziskavami protikorozijskih prevlek. Te so različnih debelin, od nekaj nanometrov debelih pasivnih tankih plasti do nekaj mikronov debelih prevlek za zaščito na visokih temperaturah. Za analizo protikorozijskih plasti se uporabljajo različne metode površinske analize, ki so prikazane v članku, kakor tudi primeri z različnih področij korozije.

Ključne besede: korozija, visokotemperaturna korozija, metode površinske analitike

1 Introduction

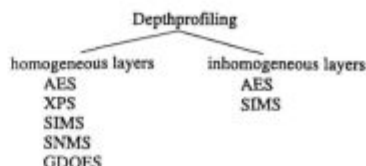
A metal is normally described as being passive, if for the existing surrounding atmosphere a high corrosion rate would be expected, instead of the very low corrosion rate to be observed. This passivity is caused by very thin dense oxide (and/or hydroxide) layers which are formed on the metal by the corrosion process. In order to get a better understanding on the effect of those passive layers they have to be analysed with respect to composition and thickness by very surface sensitive methods. High temperature oxidation and corrosion can cause great problems in power plants, petrochemical and chemical industry. A very important precondition for the practical application of a metallic material at high temperature is its oxidation or high temperature corrosion resistance. This precondition may be fulfilled if on the surface of the material protecting oxide layers are formed. These oxide layers can grow under use of the material by reaction of the material elements with the surrounding oxygen atmosphere or by a specific preoxidation at suitable temperatures in oxygen containing atmospheres. The protecting effect of those oxide layers relies on their property to act as a diffusion barrier between the metallic

and the corrosive atmosphere surrounding it. Oxide layers therefore have a key function for the application of materials in high temperature technology and there is a great need for doing research and testing the materials for such applications.

2 Methods

In order to study the growth mechanisms, nature and properties of corrosion protecting layers thin films have to be analysed spreading over a large range of thicknesses, from a few nm's for the passive layers up to several tenth of μm 's for the protecting layers on high temperature materials.

To analyse thin films with respect to layer composition and thickness different depth profiling methods can be applied depending on the thickness of the layer under study and on various sample preparation methods. Following the mainly applied surface analytical methods to be used for depth profiling of homogeneous and inhomogeneous surface layers are listed.



¹ Dr. Sc. H. VIEFFHAUS
Max-Planck-Institut für Eisenforschung GmbH
40074 Düsseldorf, Postfach 140 444 Germany

AES is Auger electron spectroscopy, XPS is X-ray excited photoelectron spectroscopy, SIMS is secondary ion mass spectroscopy, SNMS is secondary neutrals mass spectroscopy and GDOES is glow discharge optical emission spectroscopy.

To analyse inhomogeneous surface layers laterally resolving methods like AES and SIMS have to be applied. For this paper a restriction to the electron spectroscopic methods will be carried out. More detailed information on the application of the remaining methods may be found elsewhere¹.

To get a depth profile in most cases destruction of the layer to be analysed has to be performed by one of the following methods:

- a) Sputter depth profiling
- b) Angle lapping
- c) Crater edge profiling
- d) ball cratering

For sputter depth profiling the layer is decomposed by bombardment with noble gas ions and parallel or successive analysis of the momentary interface by a surface analytical method is carried out.

Angle lapping means that by using normal metal polishing equipment a layer covered sample is polished under a very flat angle. Using polishing angles down to about 1° a spreading of the surface layer up to a factor of about 100 is possible and this spreaded part of the layer may be analysed after transfer into a surface analytical system by AES point or line analysis for example.

For crater edge profiling the crater edge resulting from ion beam etching accompanying a single sputter depth profile is exploited. The crater edge of such a profile exposes the strata of the interface in a manner related to that produced by angle lapping, but the striking difference is that for crater edge profiling the resulting angles between surface and interface are 3 orders of magnitude less.

In the case of ball cratering a rotating, spherical, steel ball coated with fine diamond paste, is used to grind a spherical crater into the sample surface and after that the sample is transferred into the surface analytical system to analyse the sputter cleaned crater walls.

Advantages and disadvantages of the different methods are discussed in some detail in².

3 Results

a) Very thin surface layers (passive layers)

The only nondestructive method to depth profile very thin surface films is by angle dependent XPS - or AES - measurements. The first example to be presented concerns an oxide layer which was formed at room temperature in air on a pure zinc sample. The thickness of this layer was assumed to be only a few nm's and it should be less than the information depth of the applied electron spectroscopic methods AES or XPS.

The next **figure 1** compares the Zn - LMM Auger spectrum of a clean zinc sample (sputter cleaned by Ar⁺ ion bombardment) with the same sample after oxidation at room temperature in air. The comparison makes clear that for the oxidized sample additional features can be recognized if the analyser energy resolution is adequate (0.05%).

XPS studies on the same sample lead to the results that also for the Zn 3d- and Zn 2p- photoelectron signals a distinction between metal and oxide is possible, but the difference is most pronounced for the Zn - LMM Auger signal (in this case X-ray excited), **figure 2**.

If the information depth for the Zn - LMM Auger signal corresponding to the oxidized state of Zn is less than the thickness of the oxide layer, angle dependent measurements should reveal a more pronounced oxide signal at lower angles of analysis. This is illustrated by **figure 3**. The results of an angle dependent measurement on the X-ray excited Zn - LMM Auger signal are depicted in **figure 4** and clearly demonstrate, for angles of analysis ranging from 25° to 90°, that the information depth is less than the thickness of the oxide layer.

For a smooth, homogeneous, contamination free thin oxide layer the measured signals of the metallic and oxide components may be used to determine the oxide thickness according to equation (1):

$$\frac{I_m}{I_{ox}} = \frac{N_m}{N_{ox}} \times \frac{\lambda_m}{\lambda_{ox}} \times \frac{\exp[-d / \lambda_{ox} \sin\beta]}{1 - \exp[-d / \lambda_{ox} \sin\beta]} \quad (1)$$

where I_m , I_{ox} are the intensities of the metal and oxide signals, N_m , N_{ox} are the densities of the metal and the oxide, λ_m , λ_{ox} are the inelastic mean free paths of the Auger electrons in the metal and in the oxide, β is the angle of analysis in relation to the sample surface, see **figure 3**.

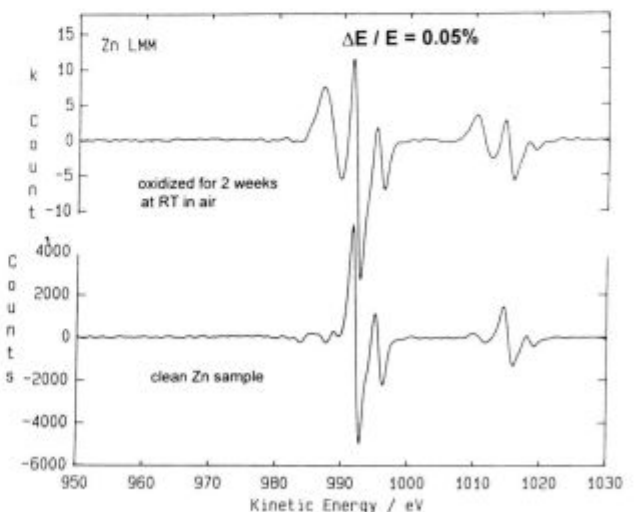


Figure 1: Comparison of the Zn - LMM - Auger spectrum for a clean zinc sample and after oxidation at room temperature in air for 2 weeks
Slika 1: Primerjava AES spektrov čistega Zn - LMM pred in po oksidaciji dva tedna na zraku pri sobni temperaturi

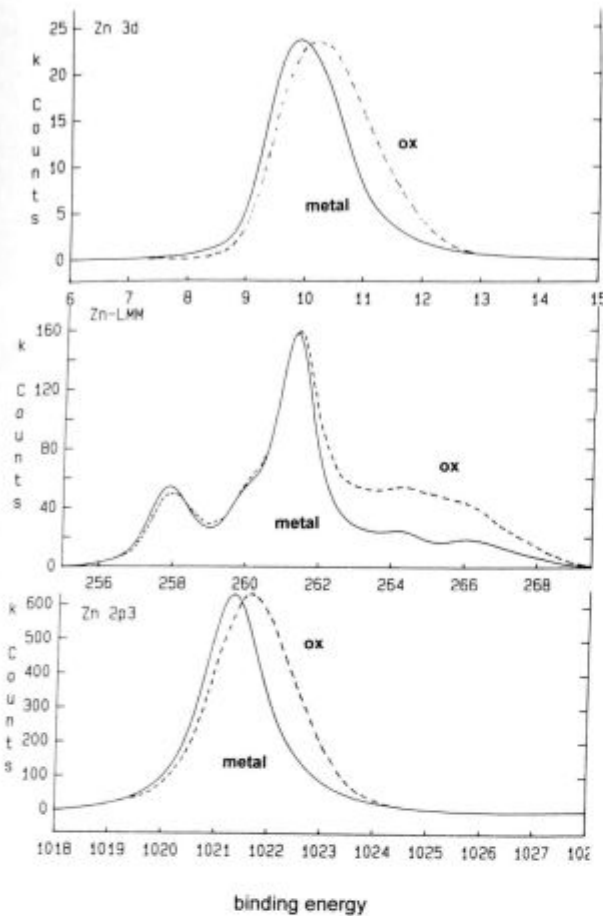


Figure 2: Zn - 3d-, Zn - 2p - photoelectron and Zn - LMM - Auger - signal for clean and oxidized zinc sample (see figure 1)

Slika 2: Zn - 3d-, Zn - 2p XPS signal in Zn - LMM AES signal za čisti in oksidirani cink (glej sliko 1)

The above equation (1) may be changed to equation (2):

$$\frac{d}{\sin\beta} = \lambda_{ox} \ln \left[\frac{N_m}{N_{ox}} \times \frac{\lambda_m}{\lambda_{ox}} \times \frac{I_{ox}}{I_m} \right] \quad (2)$$

For a determination of the layer thickness values for the λ 's are necessary. There are no experimental data for the λ - values of zinc, therefore the corresponding λ 's of zinc and zinc oxide (of zinc hydroxide as well, which will be needed lateron) were calculated according to a relation derived by Tanuma et al.³. The calculated values are (in Å):

Table 1: The calculated λ values (in Å)

	zinc	zinc oxide	zinc hydroxide
λ^{LMM}	17.7	20	21
λ^{2p}	6.7	8	7

According to equation (2) a plot of $1/\sin\beta$ against the term on the right hand side of equation (2) should give a straight line and from the slope of this straight line the thickness may be derived.

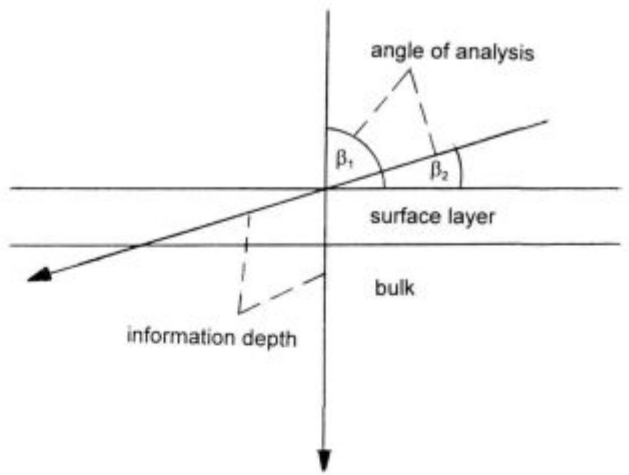


Figure 3: Schematic illustration of the higher surface sensitivity at lower angles of analysis

Slika 3: Shematični prikaz višje površinske analízne občutljivosti pri nizkih kotih

The angle dependence of the peak areas of the Zn - LMM Auger signal and the Zn - 2p photo electron signal are plotted in figure 5 for the metallic and the oxide contributions. From this plot and by using additionally the known values for N_m , N_{ox} and λ_m , λ_{ox} figure 6 can be derived. The observed straight line for the dependence of the Zn - LMM Auger signal leads to a thickness of 15Å for the oxide.

If we have a closer look to the well resolved oxygen O - 1s photo electron signal corresponding to the oxide layer, figure 7, we can detect that the assumption of a pure oxide layer was not correct, additionally to the oxide signal centered at about 530 eV peak energy a second signal caused by some hydroxide contribution is observed around 532 eV peak energy. Results of angle dependent measurements on the oxygen O - 1s signal in figure 8 indicate that we have an inner oxide layer and an outer hydroxide layer.

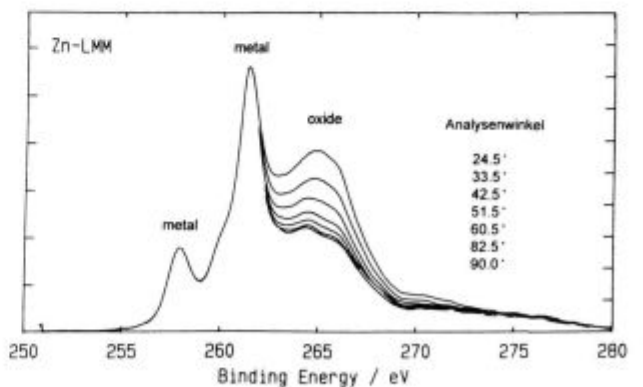


Figure 4: Angle dependence of the Zn - LMM Auger signal for an oxidized zinc sample (as for figure 1)

Slika 4: Kotna odvisnost Zn - LMM AES signala za oksidirani cink (kot na sliko 1)

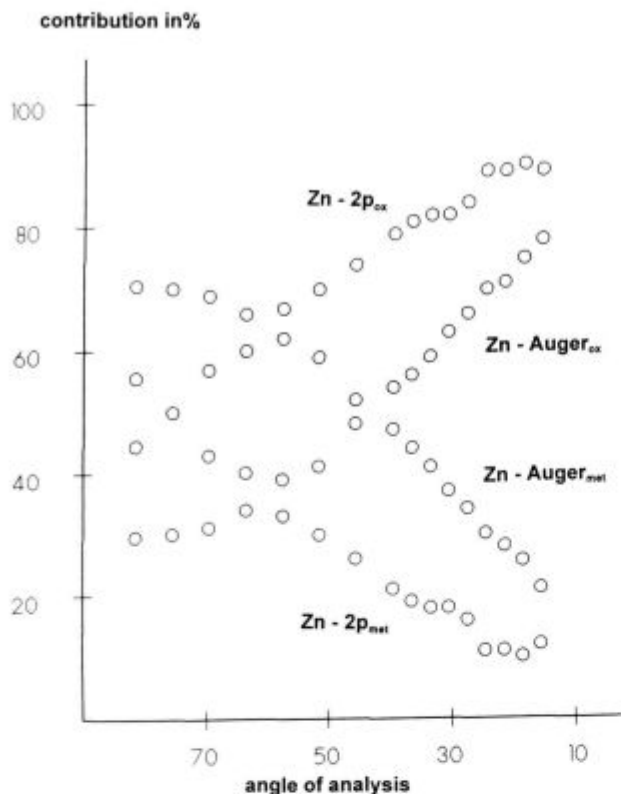


Figure 5: Angle dependence of the Zn - LMM Auger signal and Zn - 2p photoelectron signal for an oxidized zinc sample (as for figure 1), metal and oxide contributions are plotted

Slika 5: Kotna odvisnost Zn - LMM AES signala in Zn - 2p XPS signala za oksidirani cink (kot na sliki 1), prikazana sta deleža kovine in oksida

Looking more detailed to the angle dependence of the Zn - LMM Auger signal it can be recognized, figure 9, that also for this signal the "oxide" - component exhibits some peak shape variations in dependence on the angle of analysis. If we try to fit the Zn - LMM Auger signal for the oxidized sample at first, figure 10b, by a metal contribution according to figure 10a and the remaining peak area for the oxide contribution by a single peak this is not possible. We need two different peaks as shown in figure 10c, to get an acceptable fit of the whole Zn - LMM spectrum. We can now try evaluate the thickness of the oxide and the hydroxide separately.

Again we assume that the oxide and hydroxide layer are homogeneous layers. The intensity ratios of the signals of the different layers with respect to the signal of the zinc substrate are given according to S. Lecuyer et al.⁴ by:

$$\frac{I_{ZnOH}}{I_{Zn}}(\Theta) = \lambda_{ZnOH} C_{ZnOH} [1 - \exp(-\frac{d_{ZnOH}}{\lambda_{ZnOH} \cos\Theta})] / \lambda_{Zn} c_{Zn} \exp(-\frac{d_{ZnO}}{\lambda_{ZnO} \cos\Theta}) \exp(-\frac{d_{ZnOH}}{\lambda_{ZnOH} \cos\Theta}) \quad (3)$$

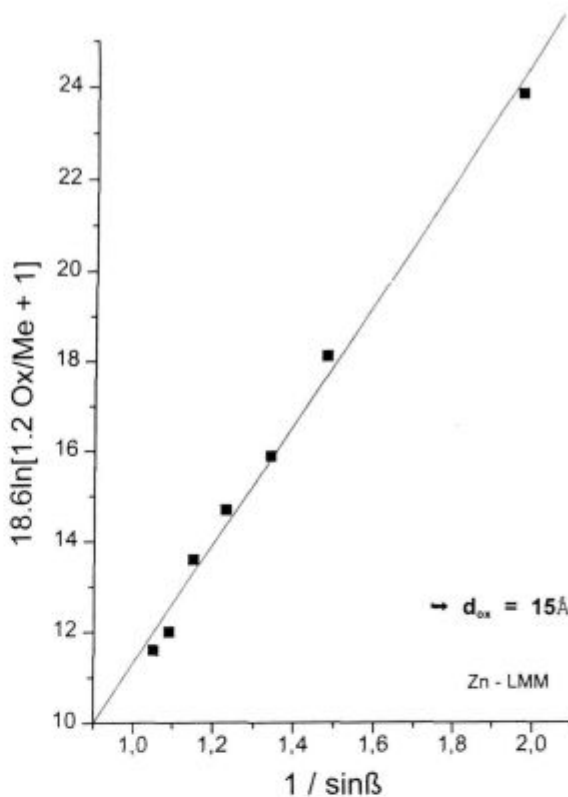


Figure 6: Determination of the oxide thickness according to equation (2), see text

Slika 6: Določitev debeline oksidne plasti po enačbi (2), glej tekst

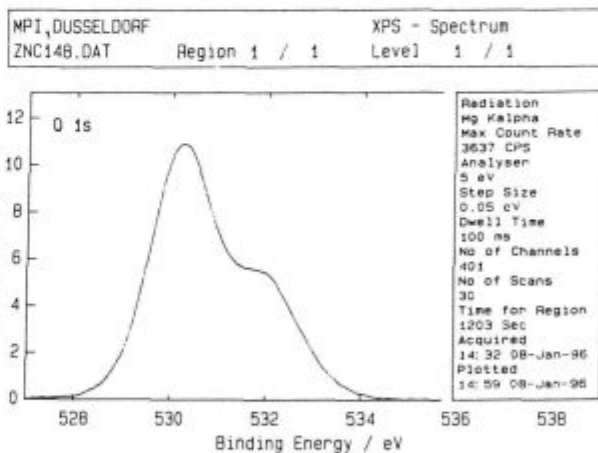


Figure 7: XPS - O - 1s signal for an oxidized zinc sample (as for figure 1)

Slika 7: XPS - O - 1s signal za oksidirani vzorec cinka (kot na sliki 1)

$$\frac{I_{ZnO}}{I_{Zn}}(\Theta) = \lambda_{ZnO} C_{ZnO} [1 - \exp(-\frac{d_{ZnO}}{\lambda_{ZnO} \cos\Theta})] / \lambda_{Zn} c_{Zn} \exp(-\frac{d_{ZnO}}{\lambda_{ZnO} \cos\Theta}) \quad (4)$$

where c_i is the concentration within layer i and d_i is the layer thickness.

For all the angle dependent measurements of the Zn - LMM Auger signal recorded for the oxidized zinc sam-

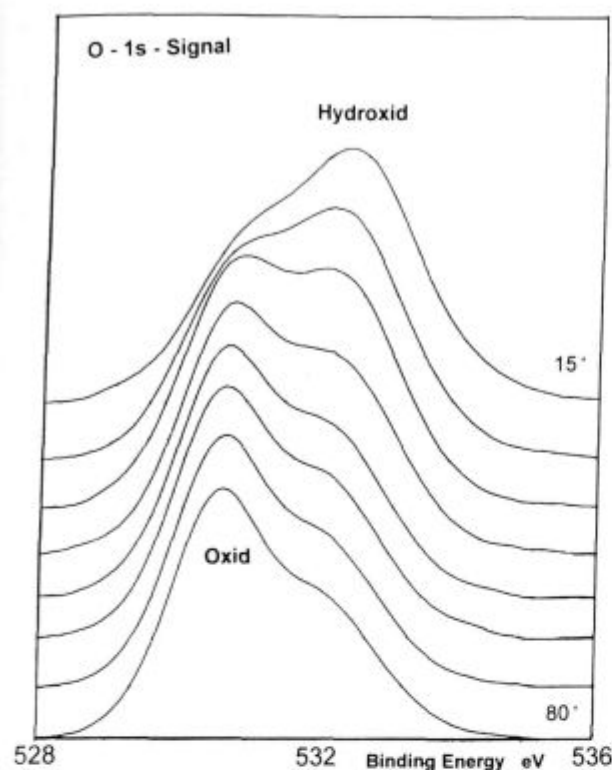


Figure 8: Angle dependent measurements for the XPS - O - 1s signal of an oxidized zinc sample (as for figure 1)

Slika 8: Meritve XPS - O - 1s signala za oksidirani vzorec cinka (kot na sliki 1) v odvisnosti od kota

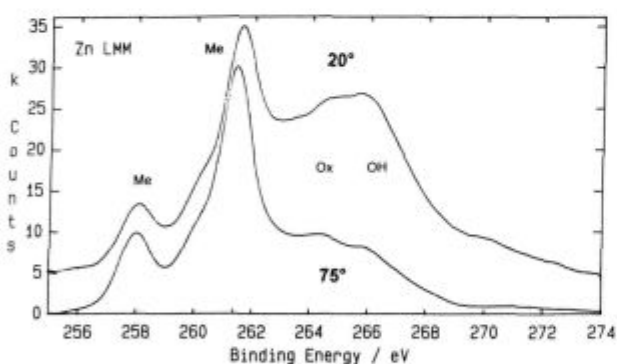


Figure 9: Zn - LMM Auger signal for an oxidized zinc sample (as for figure 1) recorded at 20° and 75° angle of analysis

Slika 9: Zn - LMM AES signal oksidirane cinka (kot na sliki 1) posnet pri kotih analize 20° in 75°

ple a peak fitting for the total LMM signal was performed in a similar way as discussed before. The measured peak area ratios I_{Ox}/I_{Me} and I_{OH}/I_{Me} for the oxide and the hydroxide layer in dependence on the angle of analysis $\tilde{Z}N1 = 0$ are listed in the table 2 together with the same peak area ratios calculated according to equation (3) and (4) by using a thickness of 13Å for the oxide layer and a thickness of 4Å for the hydroxide layer.

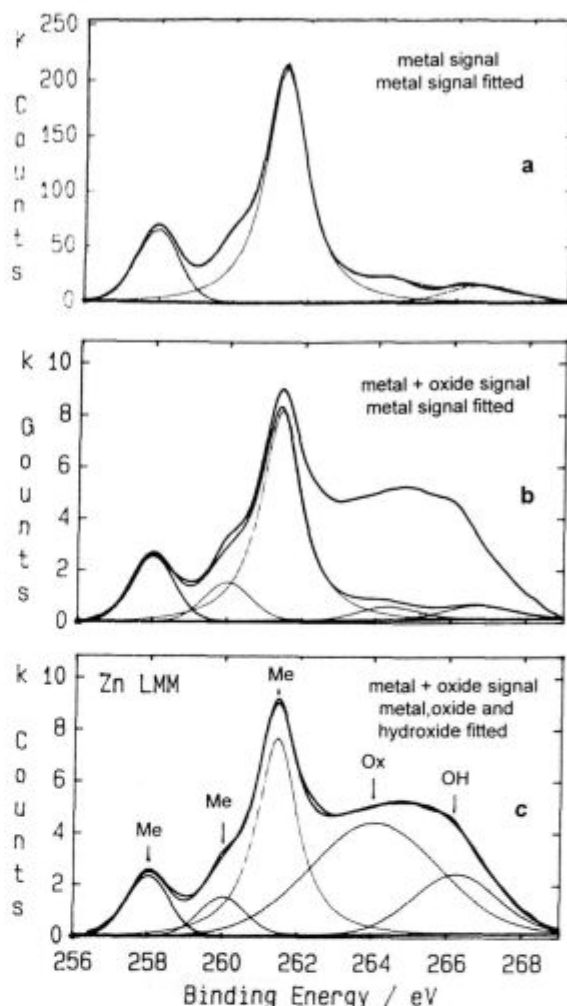


Figure 10: a) Zn - LMM Auger signal for a clean zinc sample, metal signal fitted; b) Zn - LMM Auger signal for an oxidized zinc sample (as for figure 1), metal part fitted; c) Zn - LMM Auger signal for an oxidized zinc sample (as for figure 1), metal oxide and hydroxide parts fitted

Slika 10: a) Zn - LMM AES signal za čisti cink; b) Zn - LMM AES signal za oksidirani cink (kot na sliki 1) kovinski del se prilega; c) Zn - LMM AES signal za oksidirani cink (kot na sliki 1) kovinski in hidroksidni del se prilega krivulji

Table 2: The angle dependent measurements of the Zn - LMM Auger signal for the oxide and hydroxide layer

Θ	I_{Ox}/I_{Me} (exp.)	I_{Ox}/I_{Me} (calc.)	I_{OH}/I_{Me} (exp.)	I_{OH}/I_{Me} (calc.)
78.1	13	14.7	11.7	10.5
76	9	9.05	5.8	4.1
73	5.6	5.44	2.8	2.2
70.5	3.5	3.9	1.8	1.65
68	3.15	3.1	1.25	1.05
64	2.3	2.25	0.8	0.7
60.5	1.9	1.8	0.6	0.54
58	1.5	1.6	0.5	0.42
45.4	1	1	0.25	0.28
32.9	0.79	0.77	0.18	0.18
21.4	0.65	0.67	0.15	0.17
13	0.66	0.63	0.14	0.14

For the first thickness determination, assuming a single oxide layer, a thickness of 15Å resulted, which is in very good agreement with a thickness of 17Å for the double layer consisting of a 13Å thick oxide and a 4Å thick hydroxide layer.

b) Thick layers (high temperature oxidation)

For future power plants high strength 9% Cr steels are being considered as construction materials for steam piping, headers and superheater tubes up to 600°C. For those materials it was found that the destruction of the protective oxide scale occurs during exposure in simulated combustion gas by the presence of water vapour. Although this detrimental effect of water vapour on the oxidation resistance of ferritic Cr - steels is known already for a long time no conclusive mechanism has been elucidated.

According to **figure 11**, illustrating schematically the variation with alloy Cr content of the oxidation rate and oxide scale structure, several different oxides are expected to appear for a Fe 9% Cr alloy and the above mentioned oxidation conditions.

The Fe 9% Cr alloys were oxidized isothermally in N₂ - 1% O₂ with and without various H₂O contents at 650°C. Using the crater ball equipment a crater was ground into the different oxidized samples. The crater ball process is illustrated in **figure 12**. After transferring

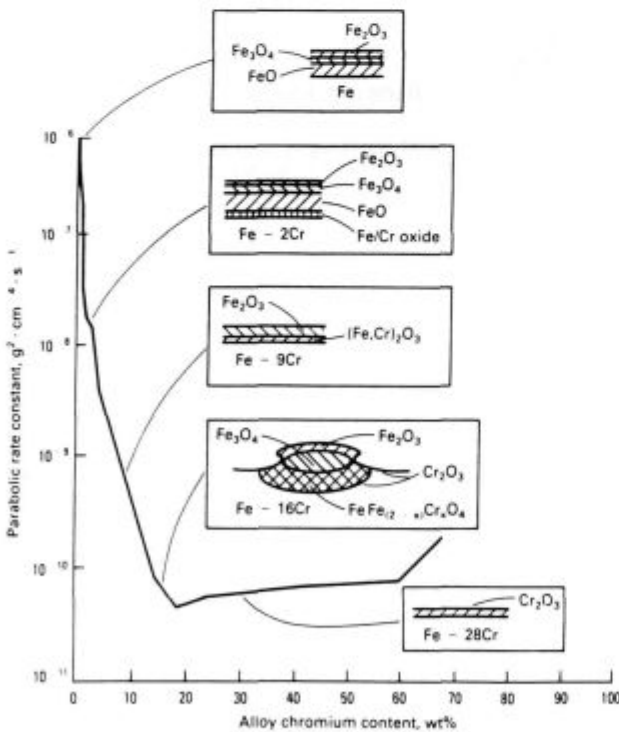


Figure 11: Schematics of the variation with alloy chromium content of the oxidation rate and oxide scale structure (based on isothermal studies at 1000°C in 0.13 atm oxygen)

Slika 11: Shematičen prikaz vpliva različnih vsebnosti kroma na stopnjo oksidacije in struktura oksida (izotermna oksidacija pri 1000°C in 0.13 atm kisika)

the samples into the scanning Auger system the samples were sputter cleaned and SEM images recorded. Two examples will be presented to show the possibilities of this method. The first sample was oxidized in N₂ - 1% O₂ - 4% H₂O at 650°C for 3 hours and the second one for 10 hours, **figure 13 to 16**.

For the application of high temperature materials the formation of even, slow growing and well adherend oxide layers are desired. Al₂O₃ layers would be the thermodynamically most stable layers for nearly all conditions occurring during the use of the material. Quite often however the nucleation and adherence of the Al₂O₃ layers are not satisfactory. The improve the adherence of those layers oxidation of a model alloy Fe - 6% Al - 0,5% Ti and 50 to 100 ppm C were studied.

After oxidation of this alloy the samples were investigated by surface analytical methods. The oxide layers were fine grained, well adherent and represented an excellent protection against carburizing atmospheres. This was tested by long term investigations.

In order to find out the reason for this improvement of the protecting properties Auger depth profiles of the oxide layer on top of the model alloy were recorded. A typical example is shown in **figure 17**. The most striking feature of this depth profile is the simultaneous enrichment of carbon and titanium at the oxide metal matrix interface. This observation leads to the assumption that by formation of a TiC layer at the interface this improvement of the corrosion protecting properties could be realized.

By further detailed surface analytical investigations on a single crystal model alloy of the same composition and applying LEED (low energy electron diffraction) and AES it could be found out that on several low indexed crystal surfaces this TiC layer grows epitaxially.

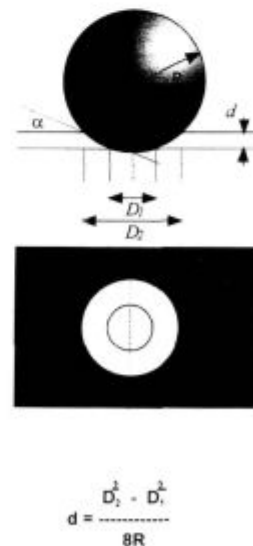


Figure 12: Schematic illustration of the crater ball etching process
Slika 12: Shematski prikaz kraterja dobljenega s procesom jedkanja s kroglico

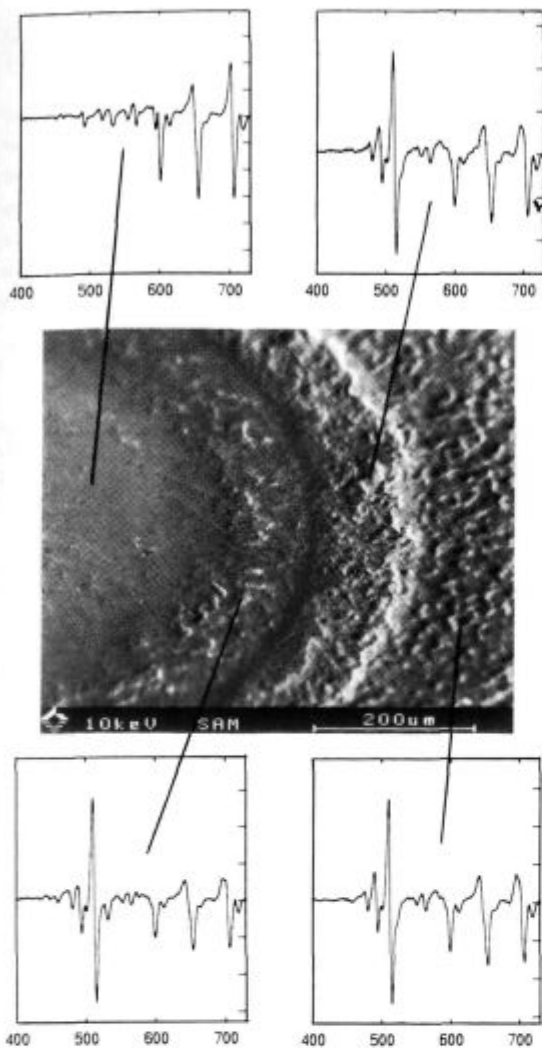


Figure 13: SEM of a part of the crater etched area of the Fe 9% Cr sample oxidized for 3 h (see text) and characteristic Auger point spectra for the different areas

Slika 13: SEM posnetek dela jedkalnega kraterja vzorca zlitine Fe 9% Cr, po 3 urah oksidacije (glej tekst) in karakteristični AES spektri, posneti na označenih mestih

Metal dusting is known to be a dangerous high temperature corrosion phenomenon in petrochemistry and in reformer and direct reduction plants. In strongly carburizing atmospheres and temperatures from 400 to 800°C low alloyed Fe, Ni and Co base alloys are subject to a catastrophic carburization leading into a desintegration of the material into a dust composed of fine metal particles and carbon. For the reaction mechanism of the metal dusting process it was assumed that instable carbides form as an intermediate before they decompose to metal and carbon dust.

In order to get a more detailed picture of the metal dusting process an iron sample from the initial stages of the metal dusting process (680°C, 78% H₂, 15% CO and 0.5% H₂O) was removed from the carburizing atmos-

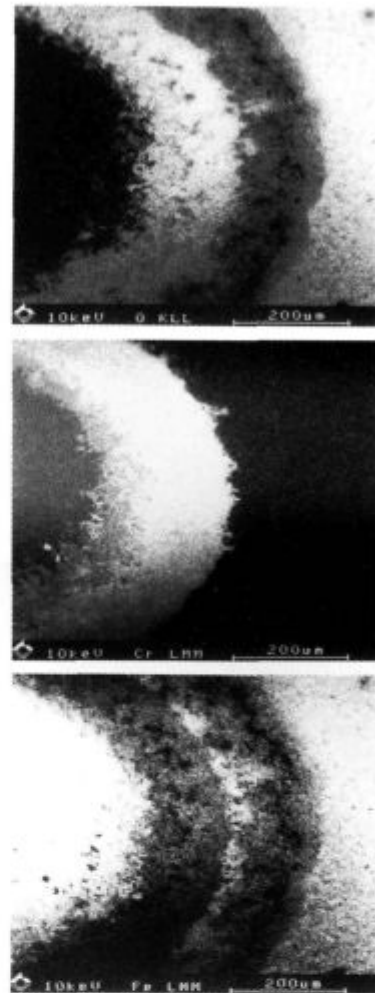


Figure 14: a) oxygen; b) chromium; c) and iron - images of the same surface area as shown in the SEM image in figure 13

Slika 14: a) kisik; b) krom; c) in železo - slike delov površin prikazanih na SEM posnetku slike 13

phere and using the crater ball equipment a crater was etched into the sample surface. After transferring the etched sample into the scanning Auger system a clean surface of the crater area was produced by Ar ion bombardement. Immediately afterwards Auger spectra and Auger images were recorded. The different chemical states of carbon within graphite and in carbide may easily be distinguished by Auger electron spectroscopy because of a characteristic Auger signal peak shape for the individual compounds. This is demonstrated by the Auger spectra in figure 18, which were recorded for different areas of the etched crater. Because of the different peak shape and a slight difference in peak energy graphite and carbide may be imaged separately. This is illustrated by the following figures, figure 19a to figure 19d, which show additional to a SEM image Auger elemental maps for carbidic carbon, carbon in graphitic form and iron of the crater region.

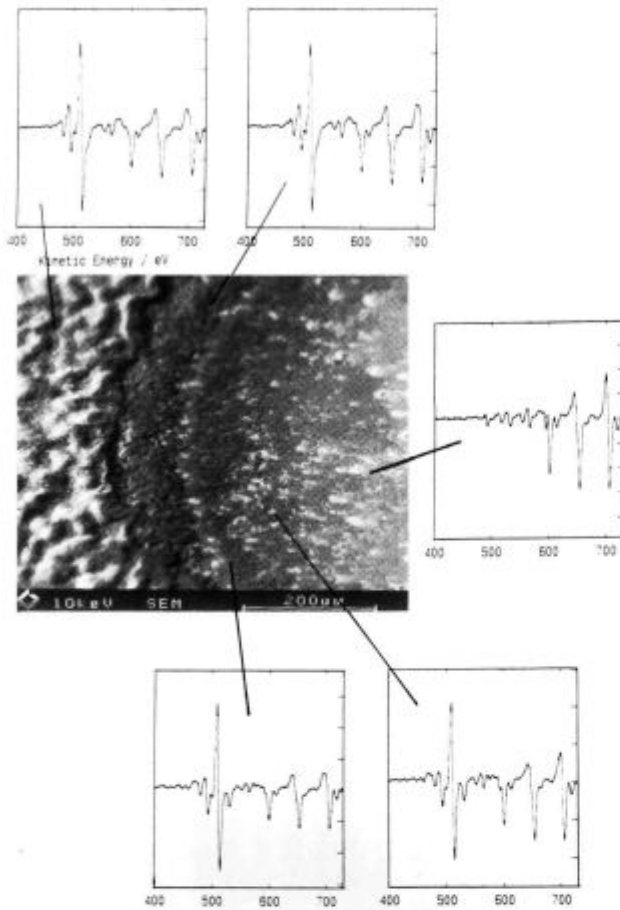


Figure 15: SEM of a part of the crater etched area of the Fe 9% Cr sample oxidized for 10 h (see text) and characteristic Auger point spectra for the different areas

Slika 15: SEM posnetek dela jedkalnega kraterja zlitine Fe 9% Cr, po 10 urah oksidacije (glej tekst) in karakteristični AES spektri, posneti na označenih mestih

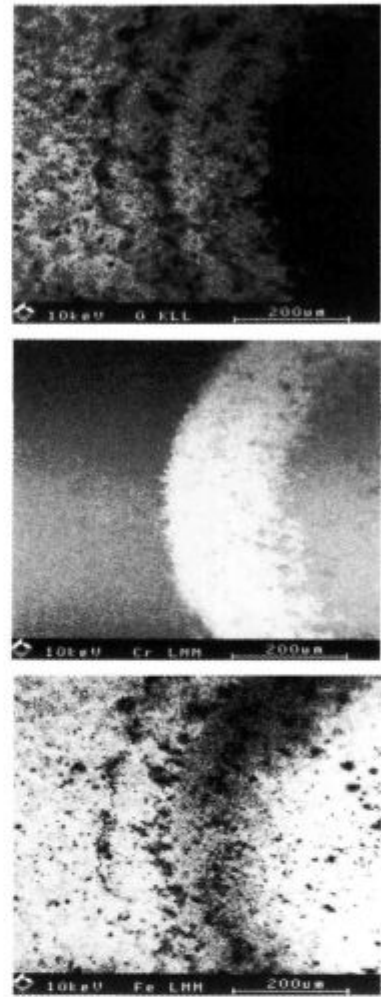


Figure 16: a) oxygen; b) chromium; c) and iron - images of the same surface area as shown in the SEM image in figure 15

Slika 16: a) kisik; b) krom; c) in železo - slike istih delov površin prikazanih na SEM posnetku slike 15

The sum up the results from different kinds of investigations the following development of surface layers during the metal dusting process can be derived (schematically):

surface metal (Fe) +C diss.	surface Fe ₃ C	surface graphite	surface coke(Fe+C)
	metal(Fe) +C diss.	Fe ₃ C	graphite
		metal(Fe) +C diss.	Fe ₃ C
			metal (Fe) +C diss.

Well adherent and corrosion protecting oxide layers are of great importance for high temperature alloys. The adherence of the oxide layers is affected by the morphology and the chemical composition of the oxide/metal interface. In this study scanning Auger microscopy (SAM) is used to investigate the oxide/alloy interface of oxidized Fe-Cr-Al alloys (undoped or doped with Ti, Ce and

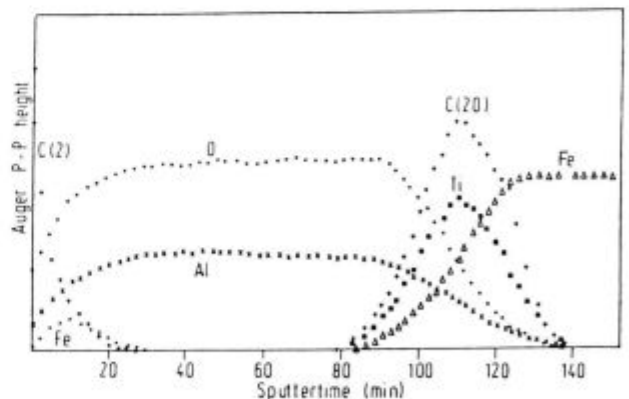


Figure 17: AES depth profile of a polycrystalline Fe-6Al-0.5Ti-0.01C sample oxidized for h at 1000°C and 10⁻¹⁹ bar oxygen partial pressure

Slika 17: AES profilni diagram polikristalne zlitine Fe-6Al-0,5Ti-0,01 C po 1/2 urni oksidaciji na temperaturi 1000°C in parcialnemu tlaku kisika 10⁻¹⁹ bar

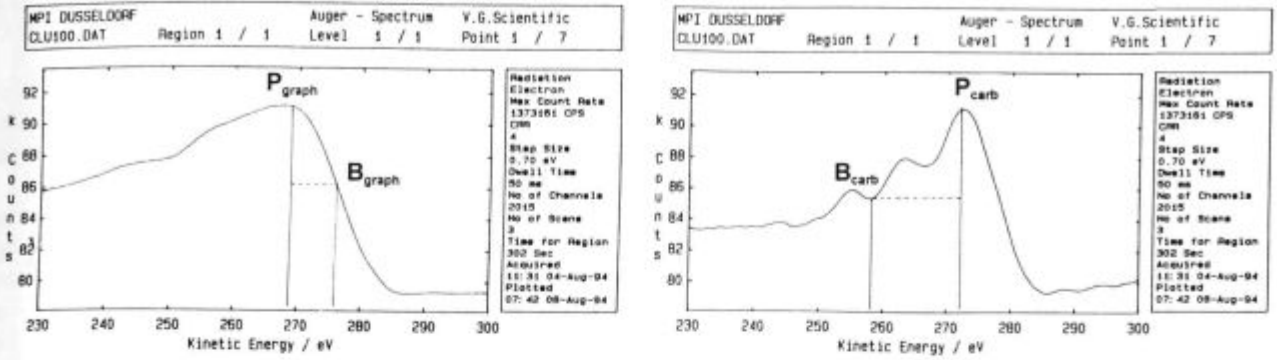


Figure 18: 'graphitic' (upper spectrum) and 'carbide' carbon - KVV Auger signal of a crater ball etched Fe metal dusting sample indicating the different peak shapes and illustrating the peak (P_i) and background (B_i) energy positions for recording the Auger images

Slika 18: 'grafitni' (zgornji spekter) in 'karbidni ogljik' - KVV Augerjev signal s kroglico jedkanega Fe prašnega vzorca z različnimi oblikami vrhov prikazuje vrh (P_i) in ozadje (B_i) in energijske pozicije za posnete AES spektre

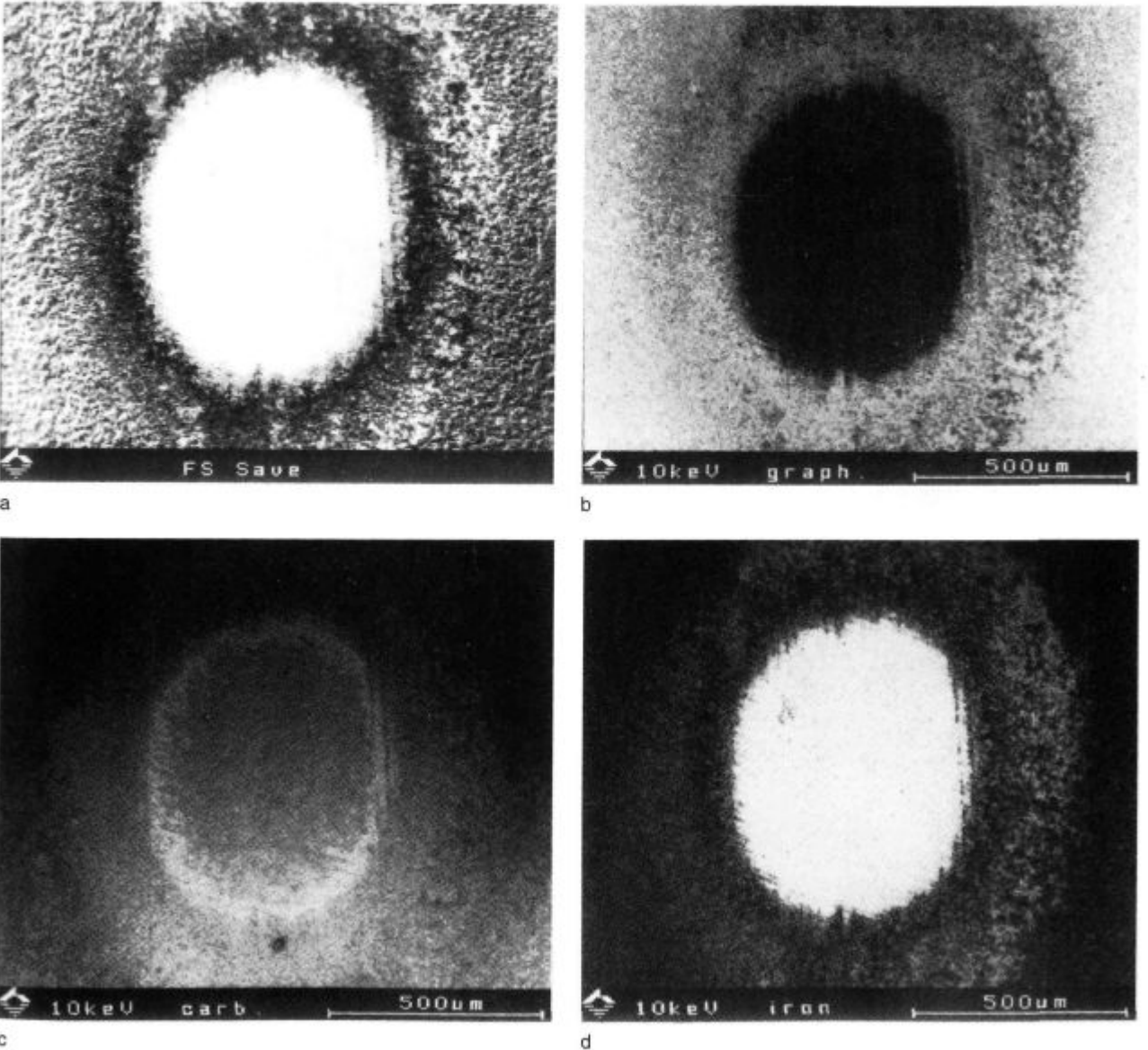
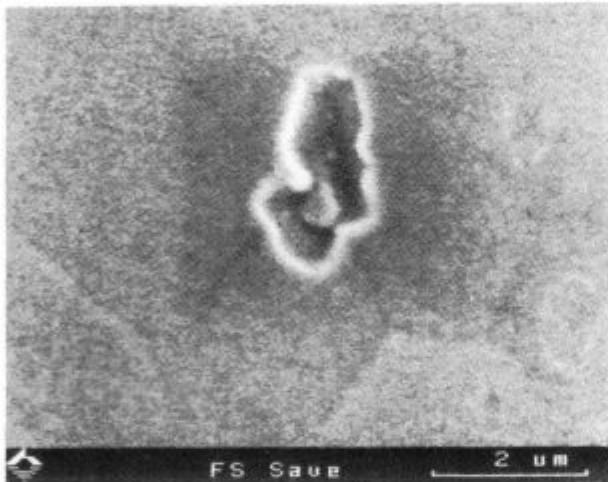


Figure 19: a) to d) SEM and SAM images of a crater ball etched and sputter cleaned Fe metal dusting sample

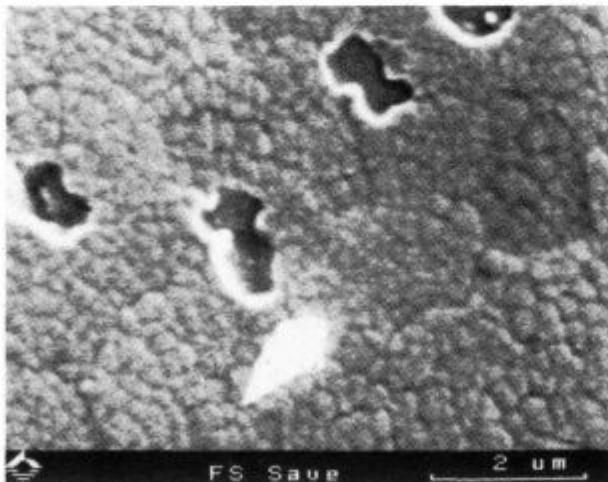
Slika 19: a) do d) SEM in SAM posnetki s kroglico jedkanega Fe prašnega vzorca in z Ar⁺ ioni jedkan Fe prašnat vzorec



a



b



c

Figure 20: a) to c) SEM images of surface areas where the oxide layer is partly (or completely) removed

Slika 20: a) do c) SEM posnetki površine, kjer je bila oksidna plast delno (ali popolnoma) odstranjena

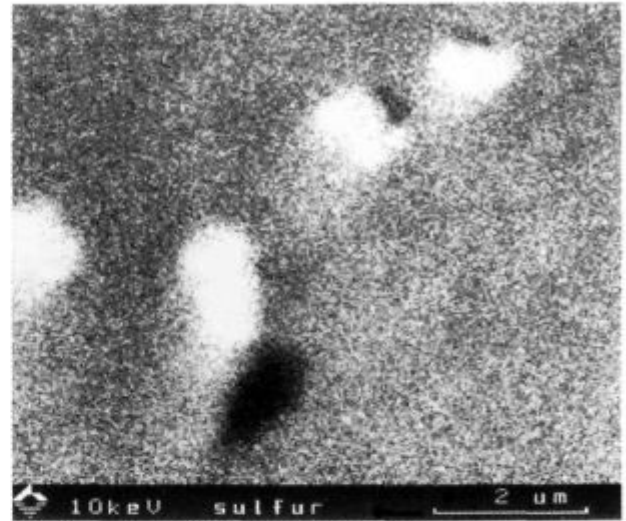


Figure 21: Sulfur image of the same surface area as shown in the SEM image of figure 20 c)

Slika 21: Posnetek žvepla na površini, prikazani na sliki 20 c)

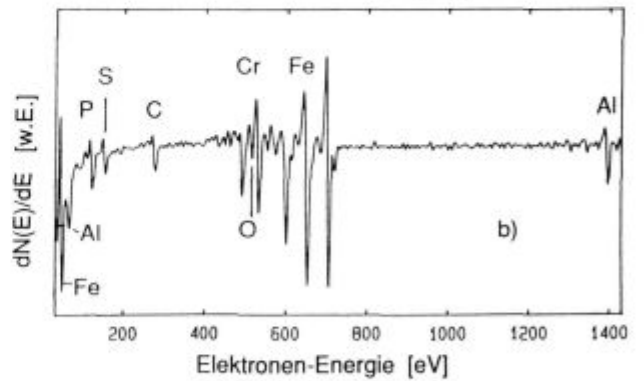
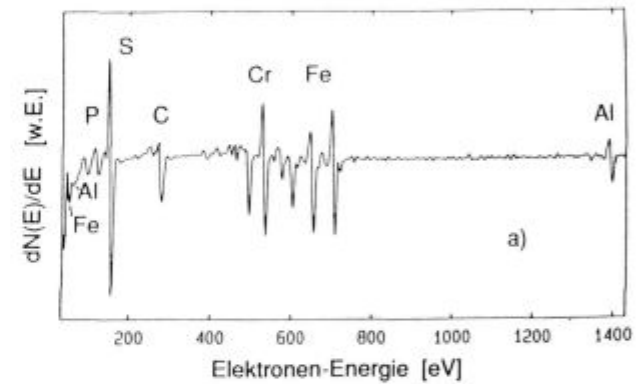


Figure 22: Auger point spectra of a) a void area; b) a rugged surface area

Slika 22: AES spekter posnet a) v vrzeli; b) na hrapavi površini

Y) after partly removing the oxide layer by in situ bending.

Thin Fe-Cr-Al ribbons, doped and undoped, were produced by meltspinning. Rectangular specimens were cut from the ribbons and ultrasonically cleaned in acetone. The samples were oxidized at 1273 K in a control-

led He - O₂ gas mixture at an oxygen partial pressure of 133 mbar.

Bending of the specimens was performed in UHV at a residual pressure of 5×10^{-9} Pa to spall off parts of the oxide layer. The stripped oxide/metal interface was investigated by in situ SEM and SAM.

The metal surface shows individual voids and rugged parts, indicating imprints of the removed oxide, see SEM figures 20a to 20c. For the undoped alloy poor adherence of the oxide layer is observed. Sulphur is strongly enriched at the surface of the voids, figure 21 shows a sulphur image of the sample area as for the SEM image in figure 20c and 22a and 22b Auger point spectra of a void surface and a rugged part of the interface.

On the Ti containing alloys the oxide layer is again poorly adherent. Sulphur is also strongly enriched at the surface of voids. On the Y- and Ce- containing alloys the oxide layer is well adherent and the sulphur concentration is below the detection limit.

The poor adherence of the oxide layers on undoped and Ti doped Fe-Cr-Al alloys is correlated to the presence of sulphur at the alloy surface. Sulphur enrichment is explained by sulphur segregation to the free alloy surface and by additional sulphide formation for the Ti containing alloys. The positive effect of Y and Ce on the ad-

herence of the oxide layers is explained by sulphide precipitation in the bulk and thus preventing sulphur segregation to the free surface of the alloy.

4 Summary

Depending on the thickness of the surface layers to be analysed by surface analytical methods with respect to composition and thickness, different methods of depth profiling have to be applied. Valuable information may be derived from the results of the surface analytical investigations, leading to a better understanding of the growth mechanisms and the corrosion protecting properties of oxide layers on metal surfaces.

5 References

- ¹ Guidelines for methods of testing and research in high temperature corrosion, European Federation of Corrosion Publications 14, The Institute of Materials, London, 1995, 189
- ² in *Practical Surface Analysis*, eds. D. Briggs and M. P. Seah, Wiley, Chichester, 1990
- ³ S. Tanuma, C. J. Powell and D. R. Penn, *Surf. Interface Anal.*, 20a, 1993, 77
- ⁴ S. Lecuyer, A. Quemerais and G. Jezequel, *Surf. Interface Anal.*, 18, 1992, 257